

## How Important Is Metal–Ligand Back-Bonding toward $YX_3$ Ligands ( $Y = N, P, C, Si$ )? An NBO Analysis

Tom Leyssens,<sup>\*,†</sup> Daniel Peeters,<sup>†</sup> A. Guy Orpen,<sup>‡</sup> and Jeremy N. Harvey<sup>\*,‡</sup>

Laboratoire de Chimie Quantique, Université Catholique de Louvain, Place Louis Pasteur 1, B-1348 Louvain-la-Neuve, Belgium, and School of Chemistry, University of Bristol, Cantock's Close, Bristol BS8 1TS, U.K.

Received December 19, 2006

An NBO second-order perturbative energy analysis is used in a quantitative study of back-bonding toward  $YX_3$  ( $Y = P, N, C, Si$ ;  $X = H, F, Me, Ph, OMe$ ) ligands as well as pyridine and bipyridine. The  $\pi$  acceptor character of these ligands in  $M-L$ ,  $L'-M-L$ , and  $M(CO)_5L$  complexes is studied at the B3LYP level of theory. All phosphine ligands are found to be  $\pi$  acceptors, whereas the  $NH_3$  and  $NMe_3$  ligands are found to be  $\sigma$ -only ligands. The NBO analysis also identifies competitive back-bonding and shows that even the carbon- and silicon-containing ligands have some  $\pi$ -bonding character.

### Introduction

Metal–ligand bonding is central to organometallic catalysis. The strength and nature of the metal–carbon bond determines the geometry and stability of the various intermediates in a catalytic cycle.<sup>1</sup> Bonding between the metal and various spectator ligands is also crucial, as it plays an important role in tuning the metal–carbon interactions. Understanding the nature of the metal–ligand bond is therefore very important.<sup>2</sup> The key aspects of bonding in metal complexes are fairly well established, with contributions from electrostatic interactions and from covalent  $\sigma$  bonding arising from donation of a ligand-based lone pair to an empty metal orbital. In some cases,  $\pi$  interactions also play a role. Ligands with  $\pi$  lone pairs can donate electrons into metal d orbitals of appropriate symmetry, whereas ligands with low-lying vacant  $\pi$  orbitals can accept electrons. This latter effect is referred to as back-bonding and is very well known for strongly  $\pi$ -accepting ligands such as carbonyl.

For some other ligands, especially the very important phosphine ligands, the existence and strength of this interaction are unclear.<sup>3</sup> As part of our work in developing a ligand knowledge base,<sup>4</sup> we are interested in using computational methods to analyze the role of back-bonding in complexes of phosphines and related  $PX_3$  phosphorus ligands. In a previous paper,<sup>5</sup> we used the electron density difference function between neutral metal complexes and the corresponding cation (in another context, this is the finite-difference Fukui function) to demonstrate that  $\pi$  back-bonding does occur even to relatively weak acceptors such as trialkyl and triaryl phosphines.<sup>6</sup> The acceptor

orbitals in this case are linear combinations of the  $P-X$  antibonding  $\sigma^*$  orbitals.<sup>7</sup> Earlier suggestions that phosphorus 3d orbitals play a role in accepting density from the metal have now been discounted.<sup>8</sup> In this study, we wish to assess the energetic impact of the back-bonding. This type of bonding forms, together with other interactions such as  $\sigma$ -bonding and electrostatic interactions, one of the major contributions to the total metal–ligand binding.

Several studies have already attempted to assess the importance of back-bonding, either by linking it to an experimentally observable quantity of the entire molecule or by breaking up the energy expression into several terms, one of which corresponds to back-bonding. The first approach can be based either on experimental work or on computation, whereas the second approach is necessarily computational. Both approaches are intrinsically rather challenging, because the real bond is a result of a combination of all effects, including  $\sigma$  and  $\pi$  bonding, and discriminating between them requires reference to hypothetical and hence somewhat arbitrary states in which one or more of these contributions has been removed.

Studies based on whole-molecule properties usually only provide insight into the relative importance of  $\pi$  bonding for a range of different phosphines. According to a structural survey of bond lengths in  $M(CO)_5L$  complexes, the trialkyl  $PMe_3$  ligand has a weak  $\pi$  acceptor character comparable to the  $PH_3$  ligand.<sup>9</sup> Another structural study based on metal–ligand bond lengths of  $Cr(CO)_4(PPh_3)L$  complexes<sup>10</sup> classifies the aryl  $PPh_3$  ligand in the same category of weak  $\pi$  acceptor phosphines, especially compared to the significantly stronger  $\pi$ -accepting  $P(OPh)_3$  ligand. The  $PF_3$  and  $PCl_3$  ligands on the other hand have the highest  $\pi$  acceptor/ $\sigma$  donor ratio, at least according to their Tolman electronic parameter, measuring the ligand electronic character,<sup>11</sup> and the  $^{13}C$  NMR data of  $LNi(CO)_3$  complexes,<sup>12</sup>

\* Corresponding authors. (T.L.) Fax: (+)32 10 47 27 07. E-mail: t.leyssens@chim.ucl.ac.be. (J.N.H.) Fax: (+)44 117 925 1295. E-mail: Jeremy.Harvey@bristol.ac.uk.

<sup>†</sup> Université Catholique de Louvain.

<sup>‡</sup> University of Bristol.

(1) Simoes, J. A. M.; Beauchamp, J. L. *Coord. Chem. Rev.* **1990**, *90*, 629–688.

(2) Frenking, G.; Frohlich, N. *Chem. Rev.* **2000**, *100*, 717–774.

(3) (a) Kuhl, O. *Coord. Chem. Rev.* **2005**, *249*, 693–704. (b) Dias, P. B.; de Piedade, M. E. M.; Simoes, J. A. M. *Coord. Chem. Rev.* **1994**, *135/136*, 737–807. (c) Tolman, C. A. *Chem. Rev.* **1977**, *77*, 313–348.

(4) Fey, N.; Tshipis, A. C.; Harris, S. E.; Harvey, J. N.; Orpen, A. G.; Mansson, R. A. *Chem.–Eur. J.* **2006**, *12*, 291–302.

(5) Leyssens, T.; Peeters, D.; Orpen, A. G.; Harvey, J. N. *New J. Chem.* **2005**, *29*, 1424–1430.

(6) (a) Orpen, A. G.; Connelly, N. G. *J. Chem. Soc., Chem. Commun.* **1985**, 1310. (b) Orpen, A. G.; Connelly, N. G. *Organometallics* **1990**, *9*, 1206.

(7) (a) Xiao, S. X.; Trogler, W. C.; Ellis, D. E.; Berkovitch-Yellin, Z. *J. Am. Chem. Soc.* **1983**, *105*, 7033. (b) Marynick, D. S. *J. Am. Chem. Soc.* **1984**, *106*, 4064. (c) Tossell, J. A.; Moore, J. H.; Giordan, J. C. *Inorg. Chem.* **1985**, *24*, 1100.

(8) Pacchioni, G.; Bagus, P. S. *Inorg. Chem.* **1992**, *31*, 4391–4398.

(9) Van Wüllen, C. *J. Comput. Chem.* **1997**, *18*, 1985–1992.

(10) Wovkulich, J. M.; Atwood, J. L.; Canada, L.; Atwood, J. D. *Organometallics* **1995**, *4*, 867–871.

as well as a photoelectron spectroscopy study of  $M(\text{CO})_5\text{L}$  complexes.<sup>13</sup>

Some “whole molecule property” studies attribute numerical values to the  $\pi$  acceptor character of the different phosphines. Within the QALE (quantitative analysis of ligand effects) approach,<sup>14</sup> the  $\pi$  acceptor parameter is estimated on the basis of the redox potentials of  $\text{MeCp}(\text{CO})_2\text{MnL}$  complexes and the  $\text{p}K_{\text{A}}$  values of the L ligands under the assumption that aryl- and alkylphosphines are  $\sigma$ -only ligands.<sup>15</sup> While this enables one to characterize the nature of more strongly  $\pi$ -accepting ligands such as phosphites, it is a questionable assumption, as shown among others by our previous work.<sup>5</sup> The  $\pi$  acceptor scale based on this technique thereby effectively contains an electronic threshold for the onset of  $\pi$  bonding. Another striking feature of this scale is the remarkable  $\pi$  acceptor ability of the  $\text{PF}_3$  ligand, classified as three times more strongly  $\pi$  accepting than the  $\text{PCl}_3$  ligand.

The “whole-molecule” approach uses an experimentally observable quantity, which is in principle due to a reorganization in  $\sigma$ ,  $\pi$ , and electrostatic bonding as well as to steric interactions, to quantify just one of these aspects. The main idea of the second approach is to avoid the potential pitfalls involved in deconvoluting all these effects by instead immediately evaluating the energetic stabilization associated with the specific back-bonding interaction. Because experimental techniques cannot probe specific bonding interactions, this requires the use of computation.

The first theoretical estimations of the back-bonding interaction in transition metal complexes were based on a decomposition of the total metal–ligand bond energy.<sup>2</sup> By using a stepwise calculation of the correct SCF bond energy, the latter can be dissected into different contributions. By identifying one of these contributions with the  $\pi$  back-bonding interaction, an indirect measure of the energetic stabilization due to this type of bonding is obtained.

The importance of the back-bonding interaction varies however according to the type of decomposition scheme used. On the basis of an extended transition state (ETS)<sup>16</sup> decomposition scheme including only the lowest unoccupied virtual orbitals,  $\pi$  back-bonding in  $\text{Fe}(\text{CO})_4\text{PR}_3$  complexes<sup>17</sup> is estimated to make a contribution to the overall bond energy of 17 to 40% (between 7 and 13 kcal/mol) of the size of the  $\sigma$  interaction. In other calculations including all virtual orbitals during the orbital relaxation step of the ETS procedure,  $\pi$  bonding was predicted to contribute between 33 and 100% (13 to 33 kcal/mol) of the impact of the  $\sigma$ -bonding term for  $\text{M}(\text{CO})_5\text{PR}_3$  complexes.<sup>18</sup> An even higher  $\pi/\sigma$  ratio is obtained by a constrained space orbital variation (CSOV) technique<sup>19</sup> applied to zerovalent metal-phosphine complexes, estimating

the  $\pi$  contribution to be 85 to 200% (9 to 20 kcal/mol) of the  $\sigma$  interaction.<sup>8</sup> The different schemes rely on slightly different procedures to decompose the overall energy change into its different contributions, which explains these discrepancies concerning the exact value of the  $\pi$  back-bonding interaction strength. However, all these methods predict a very large contribution of back-bonding to the overall bond energy.

In this study, we use a different computational approach to estimate the energetic stabilization associated with the back-bonding interaction. The natural bond orbital (NBO)<sup>20</sup> method developed by Weinhold and co-workers provides an estimate of the energy impact of secondary bonding interactions, which act as small perturbations to the total bonding. The energy contribution is derived from interactions between donor and acceptor orbitals.<sup>21</sup> This approach has been applied to a number of chemical problems, yielding chemically satisfying models accounting for effects such as the small energy difference between *cis* and *trans* difluoroethene,<sup>22</sup> the torsional barrier to rotation in ethane,<sup>23</sup> the relative stability of the isomers of the  $\text{HOI}-\text{H}_2\text{O}$  complexes,<sup>24</sup> and the properties of  $\text{X}-\text{H}$  bonds in  $\text{X}-\text{H}\cdots\text{Y}$  hydrogen bonds<sup>25</sup> for a wide range of X and Y groups. This technique can also be applied in transition metal chemistry. For example, it has been used to quantify the role of interligand  $\text{C}-\text{H}\cdots\text{C}$  hydrogen bonds in mono- and binuclear  $\text{Rh}(\text{I})$  derivatives<sup>26</sup> and to examine back-donation from  $\text{Zn}^{2+}$  to the antibonding  $\sigma^*$  C–O orbital in the  $\text{Zn}(\text{N}_2\text{H}_3\text{COO})_3^-$  complex.<sup>27</sup>

In this paper, we will use the NBO method to estimate the energy contribution of back-bonding interactions ( $\Delta E_{\text{bb}}$ ) toward  $\text{YX}_3$  ligands ( $\text{Y} = \text{C}, \text{N}, \text{Si}, \text{P}$ ). We start by discussing the different NBO-based methods available to compute donor–acceptor interactions and the overall features of the electronic structure of the compounds investigated. Our results provide a ranking of the back-bonding ability of different phosphine, phosphite, and related ligands and also allow a comparison to be made with the  $\pi$  acceptor strength of other  $\text{YX}_3$  ( $\text{Y} = \text{C}, \text{N}, \text{Si}$ ) ligands as well as other N-based ligands such as pyridines. In a final part of this paper we will compare the NBO-derived results with those from the energy decomposition schemes.

## Computational Details

All structures were optimized using Becke’s three-parameter hybrid functional (B3LYP), as implemented in the Jaguar program.<sup>28</sup> Optimized geometries are provided in the Supporting Information. For the metal atom, an effective core potential (treating relativistic

(11) Tolman, C. A. *J. Am. Chem. Soc.* **1970**, *92*, 2953–2956.

(12) Bodner, M. G.; May, M. P.; McKinney, L. E. *Inorg. Chem.* **1980**, *19*, 1951–1958.

(13) Yarbrough, L. W.; Hall, M. B. *Inorg. Chem.* **1978**, *17*, 2269–2275.

(14) (a) Rahman, M. M.; Liu, H.; Eriks, K.; Prock, A.; Giering, W. P. *Organometallics* **1989**, *8*, 1–7. (b) Rahman, M. M.; Liu, H.; Prock, A.; Giering, W. P. *Organometallics* **1987**, *6*, 650–658. (c) Liu, H.; Eriks, K.; Prock, A.; Giering, W. P. *Organometallics* **1990**, *9*, 1758–1766. (d) Fernandez, A. L.; Wilson, M. R.; Prock, A.; Giering, W. P. *Organometallics* **2001**, *20*, 3429–3435.

(15) Golovin, M. N.; Rahman, M. M.; Belmonte, J. E.; Giering, W. P. *Organometallics* **1985**, *4*, 1981–1991.

(16) Ziegler, T.; Rauk, A. *Theor. Chim. Acta* **1977**, *46*, 1. (b) Ziegler, T.; Rauk, A. *Inorg. Chem.* **1979**, *18*, 1558. (c) Ziegler, T.; Rauk, A. *Inorg. Chem.* **1979**, *18*, 1755.

(17) Gonzalez-Blanco, O.; Branchadell, V. *Organometallics* **1997**, *16*, 5556–5562.

(18) Frenking, G.; Wichmann, K.; Fröhlich, N.; Grobe, J.; Golla, W.; Le Van, D.; Krebs, B.; Läge, M. *Organometallics* **2002**, *21*, 2921–2930.

(19) (a) Bagus, P. S.; Hermann, K.; Bauschlicher, C. W. *J. Chem. Phys.* **1984**, *80*, 4378. (b) Bagus, P. S.; Hermann, K.; Bauschlicher, C. W. *J. Chem. Phys.* **1984**, *81*, 1966. (c) Bauschlicher, C. W.; Bagus, P. S.; Nelin, C. J.; Roos, B. O. *J. Chem. Phys.* **1986**, *85*, 354. (d) Hermann, K.; Bagus, P. S.; Bauschlicher, C. W. *Phys. Rev. B* **1985**, *31*, 6371.

(20) (a) Weinhold, F.; Landis, C. R. *Valency and Bonding: A Natural Bond Orbital Donor-Acceptor Perspective*; Cambridge U. Press, 2005. (b) Reed, A. E.; Weinstock, R. B.; Weinhold, F. *J. Chem. Phys.* **1985**, *83*, 735. (c) Reed, A. E.; Weinhold, F. *J. Chem. Phys.* **1985**, *83*, 1736. (d) A. E.; Reed; Curtiss, L. A.; Weinhold, F. *Chem. Rev.* **1988**, *88*, 899.

(21) (a) Kwon, O.; Sevin, F.; Mckee, M. L. *J. Phys. Chem. A* **2001**, *105*, 913–922. (b) Can, H.; Zhan, D.; Balci, M.; Brickmann, J. *Eur. J. Org. Chem.* **2003**, 1111–1117. (c) Monajjemi, M.; Chahkandi, B. *J. Mol. Struct. (THEOCHEM)* **2005**, *714*, 43–60.

(22) To be found at [http://www.chem.wisc.edu/~nbo5/tut\\_del.htm](http://www.chem.wisc.edu/~nbo5/tut_del.htm).

(23) Weinhold, F. *Angew. Chem., Int. Ed.* **2003**, *42*, 4188–4194.

(24) Sun, Q.; Li, Z.; Zeng, X.; Ge, M.; Wang, D. *J. Mol. Struct. (THEOCHEM)* **2005**, *724*, 155–161.

(25) Sosa, G. L.; Peruchena, M.; Contreras, R. H.; Castro, E. A. *J. Mol. Struct. (THEOCHEM)* **2002**, *577*, 219–228.

(26) Orian, L.; Ganis, P.; Santi, S.; Cecon, A. *J. Organomet. Chem.* **2005**, *690*, 482–492.

(27) Jesih, A.; Rahten, A.; Benkic, P.; Skapin, T.; Pejov, L.; Petrusevski, V. M. *J. Solid State Chem.* **2004**, *177*, 4482–4493.

(28) *Jaguar 5.0*; Schrödinger, L.L.C.: Portland, OR, 1991–2003.

effects for Mo and Tc) was used to represent all but the valence  $nd$  and  $(n+1)s$  and outer core  $ns$  and  $np$  electrons.<sup>29</sup> The latter were described with a triple- $\zeta$  contraction of the original double- $\zeta$  basis set; this combination is referred to as the LACV3P basis set. All nonmetal atoms were described using the standard 6-31G(d) basis set (with only the five spherical harmonic d functions).

Second-order perturbative NBO analysis is used to estimate the metal–ligand back-bonding interaction energy ( $\Delta E_{bb}$ ). Careful choice of the reference valence-bond orbital occupation pattern for the NBO analysis is necessary in order to obtain meaningful and comparable results. Our choice of reference configuration is discussed below. The overall energy  $\Delta E_{bb}$  is obtained by summing up all second-order perturbation interactions ( $E(2)$  terms) between the NBO metal donor orbitals and the relevant ligand acceptor orbitals. Briefly, the donor orbitals include the metal-based singly or doubly occupied d orbitals on the metal atom, whereas the acceptor orbitals include the X–Y  $\sigma^*$  orbitals for  $XY_3$  ligands and the N–C  $\sigma^*$  and  $\pi^*$  orbitals for pyridine ligands. A detailed list of the donor/acceptor orbital interactions considered for the determination of  $\Delta E_{bb}$  is given in the Supporting Information for each complex.

The ADF program<sup>30</sup> was used to estimate the ETS energy partitioning of the  $M(\text{CO})_5\text{YH}_3$  ( $M = \text{Cr, Mo}$ ;  $Y = \text{N, P}$ ) molecules at their B3LYP geometry, using a VWN<sup>31</sup> local exchange–correlation functional with additional gradient corrections to this functional developed by Becke<sup>32</sup> and Perdew.<sup>33</sup> A core double- $\zeta$ , valence triple- $\zeta$  quality basis set with single polarization functions for Mo and double polarization functions for all other atoms was used with a frozen core shell up to 2p for Cr and up to 3d for Mo.

## Results and Discussion

NBO analysis is based on a method for optimally expressing a given wavefunction into a localized form. The overall density matrix is transformed to give localized natural bonding orbitals (or NBOs), which are centered on either one atom (“core” or “lone pair” orbitals), two atoms (“bond” orbitals), or three atoms (“delocalized bond over three centers” or “3C-bond” orbitals). The density matrix is first used to define a minimum basis of atomic orbitals, the natural atomic orbitals (or NAOs), and the NBOs are expressed as an expansion of these orbitals. The NBO orbitals are chosen in such a way as to maximize occupancy, so that delocalization effects appear as weak departures from the idealized localized Lewis structure, in which all NBOs have occupancies of exactly 2, 1, or 0.

Some features of NBO analysis for transition metal complexes need to be commented on. First, the NBOs are expanded in a minimal NAO basis including only core, valence  $nd$ , and  $(n+1)s$  orbitals, that is, neglecting the relatively low-lying  $(n+1)p$  orbitals. By construction, therefore, the reference electronic structure cannot include a significant contribution from these metal orbitals. In many textbooks, bonding in metal complexes is described as involving this p shell, e.g., through  $sp^3d^2$  or  $sp^2d$  hybridization, respectively, in octahedral or square planar complexes. At first sight, therefore, this choice of NAO basis set is a serious shortcoming.<sup>34</sup> However, it has been shown through detailed analysis of computed wavefunctions that  $(n+1)p$  orbitals make only a minor contribution,<sup>35</sup> so that NBO analysis with a reduced NAO basis set is meaningful.<sup>36</sup> Instead,

bonding in octahedral complexes mainly involves three-center four-electron bonds (also referred to as  $\omega$  bonds).<sup>20a,37</sup> Two filled  $\sigma$  orbitals on a pair of ligands lying *trans* to each other mix with an empty  $sd^2$  hybrid on the metal to provide a bonding, a nonbonding, and an antibonding set of orbitals. Electrostatic interactions typically also stabilize the complex. For square planar complexes, three-center four-electron bonding with donation from two sets of *trans* orbitals into a pair of  $sd$  hybrids also predominates.<sup>38</sup>

A more serious shortcoming is that with the default settings, the NBO program does not include any three-center four-electron bonds. These need to be specified manually to be included. For most of the complexes studied here, the default analysis leads to a poor reference configuration and to perturbation contributions that cannot be analyzed to assess the importance of back-bonding interactions. We have used the CHOOSE procedure as implemented in NBO to get a consistent reference configuration for all NBO analyses described here, with three-center four-electron bonds for all *trans* pairs of ligands.

Back-bonding energy contributions are obtained from the NBO estimates of the stabilization interactions associated with partial electron donation from the localized NBOs of the idealized Lewis structure into the empty non-Lewis orbitals, that is, with partial departure from the idealized Lewis structure description. The energy associated with these interactions can be estimated within the NBO method in two distinct ways. First, because only small departures from the Lewis structure are involved, perturbation theory can be used to estimate the stabilization energy  $E(2)$  associated with delocalization from a donor orbital  $i$  to an acceptor orbital  $j$  as  $E(2) = \Delta E_{ij} = q_i \times F(i,j)^2/(\epsilon_j - \epsilon_i)$ . In this expression,  $q_i$  is the donor orbital occupancy,  $\epsilon_i$  and  $\epsilon_j$  are the respective orbital energies, and  $F(i,j)$  is the off-diagonal Fock matrix element expressed in the NBO basis. It is also possible to calculate interaction energies by deleting specific elements or sets of elements from the NBO Fock matrix and recomputing the energy. We have tested the perturbation and deletion methods for one test case,  $\text{Mo}(\text{CO})_5\text{PH}_3$  (see Supporting Information), and find that they yield similar results, but that the perturbation method is more straightforward to use. We have therefore used the latter throughout.

### A. Back-Bonding toward $\text{PX}_3$ , $\text{NX}_3$ , and Pyridine Ligands.

A quantitative scale of  $\pi$  acceptor strength for different phosphine ligands can now be established using the second-order perturbative analysis to estimate the  $\pi$  back-bonding interaction (see Computational Details). To place in context the magnitude of back-bonding toward phosphine ligands, we also consider the amine ligands  $\text{NH}_3$  and  $\text{NMe}_3$ . We also consider nitrogen-based ligands that can act as  $\pi$  acceptors, namely,  $\text{NF}_3$ , pyridine, and bipyridine, as well as the strongly  $\pi$ -accepting CO ligand.

The simplest metal–ligand complexes contain only one metal atom and one ligand, and following other work in the field,<sup>8</sup>

(29) Hay, P. J.; Wadt, W. R. *J. Chem. Phys.* **1985**, *82*, 270.

(30) (a) Baerends, E. J.; Ellis, D. E.; Ros, P. *Chem. Phys.* **1973**, *2* (1), 41–51. (b) Versluis, L.; Ziegler, T. *J. Chem. Phys.* **1988**, *88*, 322–328.

(31) Vosko, S. H.; Wilk, L.; Nusair, M. *Can. J. Phys.* **1980**, *58*, 1200.

(32) Becke, A. D. *Phys. Rev. A* **1988**, *38*, 3098.

(33) Perdew, J. P. *Phys. Rev. B* **1986**, *33*, 8822.

(34) Maseras, F.; Morokuma, K. *Chem. Phys. Lett.* **1992**, *195*, 500–504.

(35) (a) Landis, C. R.; Cleveland, T.; Firman, T. K. *J. Am. Chem. Soc.* **1995**, *117*, 1859–1860. (b) Dobbs, K. D.; Hehre, W. J. *J. Am. Chem. Soc.* **1986**, *108*, 4663–4664. (c) Shen, M.; Schaefer, H. F.; Partridge, H. *J. Chem. Phys.* **1993**, *98*, 508–521. (d) Langhoff, S. R.; Bauschlicher, C. W. *Ann. Rev. Phys. Chem.* **1988**, *39*, 181–212.

(36) Landis, C. R.; Weinhold, F. *J. Comput. Chem.* **2006**, *28*, 198–203.

(37) (a) Landis, C. R.; Firman, T. K.; Root, D. M.; Cleveland, T. *J. Am. Chem. Soc.* **1998**, *120*, 1842–1854. (b) Firman, T. K.; Landis, C. R. *J. Am. Chem. Soc.* **1998**, *120*, 12650–12656.

(38) (a) Appleton, T. G.; Clark, H. C.; Manzer, L. E. *Coord. Chem. Rev.* **1973**, *10*, 335–422. (b) Harvey, J. N.; Heslop, K. M.; Orpen, A. G.; Pringle, P. G. *Chem. Commun.* **2003**, 278–179.

**Table 1. Back-Bonding Interaction  $\Delta E_{bb}$  (kcal/mol) toward the L Ligand in Pd–L and L'–Pd–L Complexes (L' = NH<sub>3</sub>, PH<sub>3</sub>, CO) and toward CO in OC–Pd–L Complexes (for Pd–L, the bond dissociation energy is also given in parentheses)**

	NH <sub>3</sub> PdL	PdL	PH <sub>3</sub> PdL	COPdL	CO
NMe <sub>3</sub>	2.73	2.50 (19.26)	1.40	1.91	54.98
NH <sub>3</sub>	5.68	4.29 (23.97)	2.75	2.62	54.24
C <sub>5</sub> H <sub>5</sub> N	10.13	8.29 (22.37)	5.19	4.54	54.03
NF <sub>3</sub>	30.15	21.93 (14.81)	15.65	12.09	46.86
PH <sub>3</sub>	15.97	14.91 (36.11)	11.87	9.48	42.64
PPh <sub>3</sub>	16.91	15.38 (40.72)	11.91	9.52	46.09
PMe <sub>3</sub>	17.41	16.44 (42.03)	12.55	10.04	46.08
P(OMe)	20.12	18.31 (40.36)	14.58	11.87	43.12
PF <sub>3</sub>	26.69	23.68 (44.29)	21.93	17.38	33.88
PCl <sub>3</sub>	31.95	24.96 (37.67)	24.31	20.05	34.18
CO	54.24	50.24 (45.73)	42.64	35.12	35.12

we start by considering Pd(L), in which ligand–ligand interactions are of course absent. To assess the influence of a second ligand on bonding, we consider L'–Pd–L molecules. Table 1 shows the NBO-derived back-bonding interaction in Pd–L and L'–Pd–L complexes for a series of YX<sub>3</sub> ligands with L' = NH<sub>3</sub>, PH<sub>3</sub>, or CO. As can be seen, with very few exceptions, the  $\pi$ -acceptor character of the ligands varies in a consistent order irrespective of the nature of the second ligand: NMe<sub>3</sub> < NH<sub>3</sub> < C<sub>5</sub>H<sub>5</sub>N < PH<sub>3</sub> < PPh<sub>3</sub> < PMe<sub>3</sub> < P(OMe)<sub>3</sub> < NF<sub>3</sub> < PF<sub>3</sub> < PCl<sub>3</sub> < CO. Similar results have been reported for back-bonding in ReH<sub>3</sub>L and OsH<sub>3</sub>L (L = NH<sub>3</sub>, PH<sub>3</sub>, CO) complexes.<sup>20a</sup>

Although we observe a small stabilizing back-donating interaction toward the NH<sub>3</sub> and NMe<sub>3</sub> ligands, this  $\pi$  interaction is less than one-third of that of the corresponding PH<sub>3</sub> and PMe<sub>3</sub> ligands and 1 order of magnitude smaller than the back-bonding interaction with the CO ligand. These amine ligands are effectively  $\sigma$ -only ligands. Nevertheless, not all nitrogen-containing ligands should be considered as such. Due to the supplementary interaction with the  $\pi^*$  N–C orbital, the pyridine ligand is twice as strong a  $\pi$  acceptor as the NH<sub>3</sub> ligand, while still being much weaker in this respect than any of the phosphine ligands studied. That nitrogen-containing ligands can also have a very strong  $\pi$  acceptor character is shown by the back-bonding properties of the NF<sub>3</sub> ligand, which shows  $\pi$  back-bonding interactions comparable to those of the strong PF<sub>3</sub> and PCl<sub>3</sub>  $\pi$  acceptors. The presence of back-bonding toward the NF<sub>3</sub> ligand was verified by analysis of the finite difference Fukui function<sup>39</sup> (see Supporting Information), similar to our previous study on the nature of the metal–phosphorus bond for alkyl- and arylphosphines.<sup>5</sup>

In contrast to the amine ligands all phosphine ligands show moderate to strong  $\pi$  acceptor abilities. The PH<sub>3</sub>, PMe<sub>3</sub>, and PPh<sub>3</sub> ligands are characterized by  $\pi$ -bonding interactions three times the size of that of the amine ligands in the studied Pd complexes, clearly indicating that the aryl- and alkylphosphines are not to be considered as  $\sigma$ -only ligands, confirming our earlier work.<sup>5</sup> Table 1 shows the P(OMe)<sub>3</sub> ligand to have a slightly more important  $\pi$  acceptor character and confirms the important back-donating interaction with the PF<sub>3</sub> and PCl<sub>3</sub> ligands, with the latter being the strongest P-based  $\pi$  acceptor, confirming a theoretical NMR study on both of these ligands.<sup>40</sup> As expected, the strongest acceptor ligand overall is CO.

The magnitude of the back-bonding contribution relative to the overall bond energy is strongly dependent on the type of ligand. As expected, the back-bonding interaction for the  $\sigma$ -only

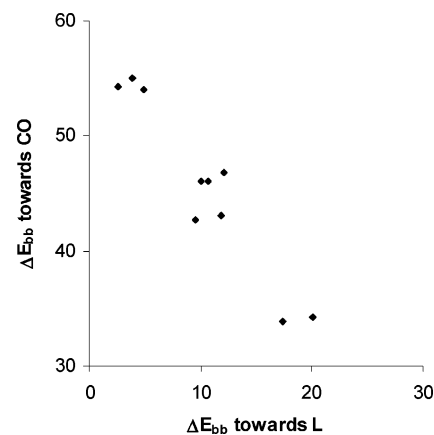


**Figure 1.** Back-bonding interaction ( $\Delta E_{bb}$ ) toward the carbonyl ligand vs back-bonding toward the L ligands in CO–Pd–L complexes (kcal/mol).

NH<sub>3</sub> and NMe<sub>3</sub> ligands represents only a small fraction of the total bonding energy (13 and 18%, respectively). For the phosphine ligands, the contribution from back-bonding is much larger both in absolute and in relative terms, contributing from 37 to nearly 70% of the total bonding energy. For the NF<sub>3</sub> and CO ligands, the back-bonding interaction is actually *larger* than the total bond energy (21.93 vs 14.81 and 50.24 vs 45.73 kcal/mol, respectively). This suggests that the structure of these compounds is partly driven by the strong back-bonding interaction and that the sum of the other interactions (electrostatic and Pauli interactions as well as  $\sigma$ -donation) may be very weakly bonding or even nonbonding at the equilibrium geometry.

When a ligand is added to a metal atom, the electronic distribution around the metal atom will change due to the specific  $\sigma$ - and  $\pi$ -bonding properties of the added ligand. The bonding interactions with any other ligand that was already linked to the metal atom will consequently also change. In order to study the influence of an added ligand on the  $\pi$  back-bonding interaction, we compare the back-bonding interaction toward an L ligand in a monosubstituted Pd–L complex with the back-bonding toward L in a bi-substituted L'–Pd–L complex. As shown by Table 1, the  $\pi$  interaction between the Pd atom and a given ligand L can vary strongly with the nature of L'.

Adding a  $\sigma$ -only ligand increases the electron density around the metal atom, which will result in an increased  $\pi$  back-donation toward the L ligand, as shown by the increased  $\pi$  interaction for the H<sub>3</sub>N–Pd–L complexes. For L' ligands that are also  $\pi$  acceptors, the opposite is observed. This is due to competition for back-bonding from the same metal d orbital between the L and L' ligand. Hence back-bonding to L is weaker in H<sub>3</sub>P–Pd–L and OC–Pd–L complexes than in Pd–L complexes.

The magnitude of the decrease in  $\pi$  bonding depends on the nature of L'. The strongly  $\pi$ -accepting CO ligand affects the back-bonding more than the weaker PH<sub>3</sub>  $\pi$  acceptor. Up to half of the metal–L  $\pi$ -bonding interaction can be lost when a CO ligand is added to the Pd–L complex. In turn the back-bonding interaction toward the two  $\pi^*$  C–O orbitals of the CO ligand is also affected by the nature of the second ligand attached to the complex, as can be seen for the various CO–Pd–L complexes. As shown by Table 1 and Figure 1, the ligands L that are stronger  $\pi$  acceptors will lead to a weaker back-bonding interaction with the CO ligand, consistent with the chemical idea of two *trans* ligands competing for the same metal d orbitals. The CO  $\pi$  interaction can decrease by as much as 20 kcal/mol relative to the Pd–CO complex, depending on the

(39) Parr, R. G.; Yang, W. *J. Am. Chem. Soc.* **1984**, *106*, 4049.

(40) Ruiz-Morales, Y.; Ziegler, T. *J. Phys. Chem. A* **1998**, *102*, 3970–3976.

**Table 2.** Back-Bonding Interaction,  $\Delta E_{bb}$  (kcal/mol), toward the L Ligand for  $M(\text{CO})_5\text{L}$  Complexes ( $M = \text{Cr}, \text{Mo}$ )

	NMe <sub>3</sub>	NH <sub>3</sub>	C <sub>5</sub> H <sub>5</sub> N	NF <sub>3</sub>	bipy <sup>a</sup>	2*py <sup>a</sup>
Cr	0.10	0.37	4.41	13.34	16.20	11.56
Mo	0.80	0.79	8.73	18.21	27.51	22.70

	PH <sub>3</sub>	PPh <sub>3</sub>	PMe <sub>3</sub>	P(OMe) <sub>3</sub>	PF <sub>3</sub>	PCl <sub>3</sub>	CO
Cr	4.37	3.10	3.62	5.35	11.92	15.74	35.13
Mo	6.56	6.48	6.92	8.88	16.87	23.97	52.27

<sup>a</sup>  $M(\text{CO})_4\text{L}$  complexes.

nature of L. This decreased stabilization with respect to metal–CO  $\pi$  bonding is recovered by an increased stabilization in metal–L  $\pi$  bonding, as can be seen from the negative trend in Figure 1. Changes in the strength of the  $\sigma$  bonding may occur also but are not considered here.

The extent of  $\pi$  donation toward a given ligand is influenced not only by the number and nature of other ligands present in the complex but also by the nature of the metal atom. This can be seen by considering the importance of back-bonding for  $d^6$   $M(\text{CO})_5\text{L}$  complexes ( $M = \text{Cr}$  or  $\text{Mo}$ ), as shown in Table 2. Note that for the bipyridine and bis(pyridine) complexes, the metal fragment is  $M(\text{CO})_4$  rather than  $M(\text{CO})_5$ .

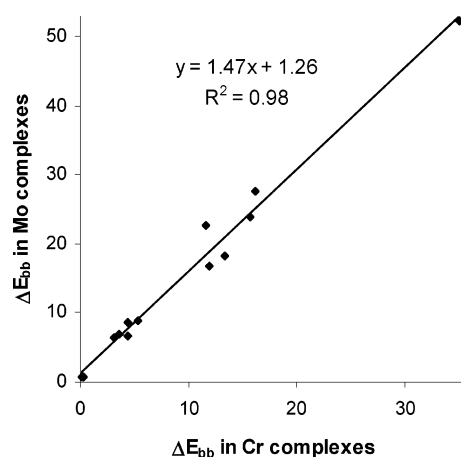
The order of  $\pi$  acceptor strength within the series of N- and P-based ligands in the Cr and Mo complexes is the same as that obtained for the simpler Pd complexes. The NH<sub>3</sub> and NMe<sub>3</sub> ligands emerge once more as  $\sigma$ -only ligands, while the NF<sub>3</sub> ligand is still characterized by a strong back-bonding interaction. The PH<sub>3</sub>, PMe<sub>3</sub>, and PPh<sub>3</sub> ligands again show some moderate  $\pi$  acceptor character. The PMe<sub>3</sub> ligand is a slightly better  $\pi$  acceptor than the PPh<sub>3</sub> ligand, which is in apparent contrast with the higher Tolman parameter for PPh<sub>3</sub>.<sup>11</sup> The Tolman parameter correlates with both the  $\sigma$  donor character of the ligand (stronger donors lead to lower C–O stretching frequency in Ni(CO)<sub>3</sub>(L)) and the  $\pi$  acceptor character (better acceptors lead to higher stretching frequencies). As PMe<sub>3</sub> is certainly a better  $\sigma$  donor than PPh<sub>3</sub>, the Tolman parameter values are consistent with it also being a slightly better  $\pi$  acceptor. P(OMe)<sub>3</sub> shows a slightly more emphasized  $\pi$  acceptor character, while PF<sub>3</sub> and PCl<sub>3</sub> once more appear as strong acceptors, although they remain weaker  $\pi$  acceptors in comparison to the CO ligand. With the exception of NF<sub>3</sub>, CO, and pyridine, all ligands have a decrease in back-bonding interaction in the  $M(\text{CO})_5\text{L}$  complexes compared to the Pd complexes studied earlier. This is due, among other factors, to a smaller number of d electrons (formal  $d^6$  instead of  $d^{10}$ ) and an increased number of CO ligands, decreasing the electron density around the metal atom.

In agreement with an experimental solvatochromism study,<sup>41</sup> Table 2 shows bipyridine to be a strong  $\pi$  acceptor, due to strong metal  $d/\pi^*$  N–C back-bonding interactions. One might expect the back-bonding interaction with bipyridine to be twice as large as for pyridine. In fact, as shown in Table 2,  $\Delta E_{bb}$  is three times larger for bipy in  $\text{Cr}(\text{CO})_4(\text{bipy})$  than for the pyridine ligand in  $\text{Cr}(\text{CO})_5(\text{py})$ . This is partly due to the increased electron density on the metal center in  $M(\text{CO})_4(\text{bipy})$  as compared to  $M(\text{CO})_5(\text{py})$  due to the presence of four instead of five CO ligands and of two instead of one  $\sigma$  donor nitrogen atoms. Indeed, the sum of the back-bonding interactions for the two pyridine ligands in *cis*- $M(\text{CO})_4(\text{py})_2$  is also nearly three times larger than the interaction in  $M(\text{CO})_5(\text{py})$ . To the extent that it is significant, the slightly higher value for the bipyridine ligand compared to

**Table 3.** Total Second-Order Perturbative Interaction between the Metal d Orbitals and Ligand Y–X  $\sigma^*$  or  $\pi^*$  Orbitals, Energy of the Respective Orbitals  $\epsilon_{\text{donor}}$  and  $\epsilon_{\text{acceptor}}$ , Energy Difference between These Orbitals ( $\Delta\epsilon$ ) and Off-Diagonal NBO Fock Matrix Element  $F(i,j)$  (kcal/mol)

L	M	$E(2)$	$\epsilon_{\text{donor}}$	$\epsilon_{\text{acceptor}}$	$\Delta\epsilon$	$F(i,j)$
PH <sub>3</sub>	Cr	2.22	–120.5	126.1	246.6	13.2
	Mo	3.30	–109.2	126.8	235.9	15.7
PF <sub>3</sub>	Cr	6.00	–136.2	61.5	197.7	18.2
	Mo	8.84	–124.2	60.9	185.1	21.3
NH <sub>3</sub>	Cr	0.22	–111.1	262.3	373.4	5.0
	Mo	0.48	–97.9	259.8	357.7	7.5
NF <sub>3</sub>	Cr	6.78	–125.5	–8.8	116.7	15.1
	Mo	9.22	–113.6	–7.5	106.0	16.9
Pyr <sup>a</sup>	Cr	0.38	–108.6	304.3	412.9	6.9
		(4.03)	(–107.3)	(–25.7)	(81.6)	(13.2)
	Mo	1.02	–96.0	302.5	398.5	11.3
		(7.71)	(–94.8)	(–27.0)	(67.8)	(16.3)

<sup>a</sup> The value in parentheses gives the data concerning the  $\pi^*$  C–N/metal  $d_{xz}$  orbital interaction.

**Figure 2.** Back-bonding interaction ( $\Delta E_{bb}$ ) toward the L ligand in Mo vs Cr complexes (kcal/mol) (data from Table 2).

the sum of the two pyridine ligands may result from improved orbital overlap due to the planar structure of the bipy ligand.<sup>42</sup>

A comparison of the back-bonding interactions of the corresponding Mo and Cr complexes in Table 2 sheds light on the importance of the nature of the metal atom. The back-bonding interaction is about 1.5 times more important for the Mo complexes compared to the Cr complexes. This is presented graphically in Figure 2 and is in agreement with earlier work.<sup>43</sup>

In order to rationalize the differences between the different complexes and ligands considered here, it is useful to consider the two factors affecting the magnitude of the back-bonding interactions, namely, the energy difference between the donor and acceptor orbitals, and the off-diagonal Fock matrix element  $F(i,j)$ . The latter is a resonance integral, measuring how much energy is gained by sharing electrons between orbitals  $i$  and  $j$ . In practice, this term can be interpreted as measuring the extent of overlap between these orbitals in physically important regions. Table 3 shows the total second-order perturbative interaction between one of the metal d orbitals ( $d_{xz}$ ) and the relevant ligand acceptor orbital as well as the energies of the corresponding NBO orbitals and the  $F(i,j)$  Fock matrix element. The geometry of the  $M(\text{CO})_5\text{YX}_3$  compounds of Table 3 is such that the M–Y axis is the  $z$ -axis, and the  $xz$  plane bisects the carbonyl ligands

(42) The two pyridine rings are slightly twisted with respect to one another in the *cis*- $M(\text{CO})_4\text{pyr}_2$  molecule.

(43) King, W. A.; Di Bella, S.; Lanza, G.; Khan, K.; Duncalf, D. J.; Cloke, F. G. N.; Fragala, I. L.; Marks, T. J. *J. Am. Chem. Soc.* **1996**, *118*, 627–635.

(41) Ernst, S.; Kurth, Y.; Kaim, W. *J. Organomet. Chem.* **1986**, *302*, 211–215.

**Table 4.** Back-Bonding  $\Delta E_{\text{bb}}$  (kcal/mol) toward the L Ligand for Anionic Pd<sup>-</sup>-L and L'-Pd<sup>-</sup>-L Complexes (L' = NH<sub>3</sub>, PH<sub>3</sub>, CO), toward the CO Ligand in Anionic OC-Pd<sup>-</sup>-L Complexes, and toward the Ligand in Neutral M(CO)<sub>5</sub>L (M = Mn, Tc) Complexes

L	H <sub>3</sub> NPd <sup>-</sup> L	Pd <sup>-</sup> L	H <sub>3</sub> PPd <sup>-</sup> L	OCPd <sup>-</sup> L <sup>a</sup>	OCPd <sup>-</sup> L <sup>b</sup>	Mn(CO) <sub>5</sub> L	Tc(CO) <sub>5</sub> L
CH <sub>3</sub>	8.68	10.23	5.01	3.96	69.10	0.00	0.70
CF <sub>3</sub>	16.23	19.05	10.33	8.77	69.42	2.75	5.20
SiH <sub>3</sub>	10.56	12.44	6.99	5.32	60.70	0.74	0.63
SiF <sub>3</sub>	11.83	13.84	7.90	6.51	55.52	1.66	1.41

<sup>a</sup>  $\Delta E_{\text{bb}}$  toward the L ligand. <sup>b</sup>  $\Delta E_{\text{bb}}$  toward the CO ligand.

and contains one of the Y-X bonds. In this orientation, the orbitals of the amine and phosphine ligands having significant interaction (>0.1 kcal/mol) with the metal d<sub>yz</sub> orbital are the two degenerate  $\sigma^*$  Y-X orbitals not lying in the xz plane. For the M(CO)<sub>5</sub>Pyr complex, the geometry is chosen such that the planar pyridine ligand lies in the yz plane. The interactions given in Table 3 for this ligand are the sum of the two  $\sigma^*$  C-N/metal d<sub>yz</sub> orbital interactions, as well as the  $\pi^*$  C-N/metal d<sub>xz</sub> orbital interaction (value in parentheses).

Table 3 shows the individual back-bonding interactions with the metal d<sub>yz</sub> orbital to be larger for the Mo complexes than for the Cr ones, as already noted for the overall interaction. This can be rationalized by the higher energy of the donor d<sub>yz</sub> orbital for Mo than for Cr, the typical energy difference being on the order of 10 kcal/mol. As expected, for a given ligand, the acceptor orbitals have similar energies in both cases. The larger 4d orbitals on Mo compared to Cr also lead to slightly larger overlap terms  $F(i,j)$ .

Although the donor orbitals are slightly lower in energy in the M(CO)<sub>5</sub>(PF<sub>3</sub>) complexes than in the corresponding PH<sub>3</sub> compounds, perhaps reflecting the weaker  $\sigma$  donor character, the tremendous lowering of the acceptor orbitals in the former species leads to an orbital gap that is roughly 50 kcal/mol smaller. This explains the much larger back-bonding interactions with PF<sub>3</sub> compared to PH<sub>3</sub>. The back-bonding interaction with PF<sub>3</sub> is also favored by better overlap between the metal donor orbital and the acceptor  $\sigma^*$  orbital. This can be understood because the P-F bond is more polar than the P-H bond, and hence the contribution of the P atom to the corresponding  $\sigma^*$  orbitals is larger.

The high energy of the  $\sigma^*$  N-H and  $\sigma^*$  N-C orbitals explains the  $\sigma$ -only character of the NH<sub>3</sub> and NMe<sub>3</sub> ligands, whereas the low-lying  $\sigma^*$  N-F orbitals are favorable for back-bonding to NF<sub>3</sub>. The  $\pi$  acceptor character of the pyridine ligand cannot be attributed to the  $\sigma^*$  N-C orbitals but is clearly due to the presence of a low-lying  $\pi^*$  C-N orbital. Only on the basis of the energy difference  $\Delta\epsilon$  between the donor and acceptor orbitals, one would expect pyridine and NF<sub>3</sub> to be stronger  $\pi$  acceptors than the PF<sub>3</sub> ligand. However, the overlap term is largest for PF<sub>3</sub>, which explains why the overall back-bonding interaction is roughly of the same magnitude for the three ligands.

**B. Back-Bonding toward CX<sub>3</sub> and SiX<sub>3</sub> Ligands (X = H, F).** In addition to the neutral ligands considered above, we have extended our NBO analysis to other YX<sub>3</sub> ligands such as the CH<sub>3</sub>, CF<sub>3</sub>, SiH<sub>3</sub>, and SiF<sub>3</sub> ligands, for which there is no clear-cut evidence whether or not to consider them as  $\pi$  acceptors. A structural survey on planar Pt(II) complexes<sup>44</sup> explains the shorter Pt-C bond length in CF<sub>3</sub> compounds compared to CH<sub>3</sub> species by an increased positive charge induced by the fluorine atoms on the carbon atoms, although stronger  $\pi$  back-bonding for the former species is also considered. An experimental carbonyl stretching frequency study on LMn(CO)<sub>5</sub> and LM(CO)<sub>5</sub> complexes attributes no  $\pi$  acceptor character to the CH<sub>3</sub> and CF<sub>3</sub> ligands.<sup>45</sup> The valence photoelectron spectra of CpFe-

(CO)<sub>2</sub>L complexes<sup>46</sup> confirm the absence of back-bonding toward the methyl ligand. A theoretical study on the relative stabilities of transition metal alkylidyne (CH<sub>3</sub>)<sub>2</sub>M(=CH)(X) and bis(alkylidene) CH<sub>3</sub>M(=CH<sub>2</sub>)<sub>2</sub> complexes<sup>47</sup> suggests that the  $\pi$  acceptor character increases in the order CH<sub>3</sub> < CF<sub>3</sub> < SiH<sub>3</sub> < SiF<sub>3</sub>. Stronger back-bonding toward halogen-silicon  $\sigma^*$  orbitals compared to other Si-X bonds is confirmed by an experimental structural, IR, and NMR study of Cp(PMe<sub>3</sub>)<sub>2</sub>-RuSiR<sub>3</sub> complexes<sup>48</sup> as well as by a theoretical NLMO/NBO analysis of Os(SiR<sub>3</sub>)Cl(CO)(PPh<sub>3</sub>)<sub>2</sub> complexes.<sup>49</sup>

We used the NBO perturbative analysis to study back-bonding in the L'-Pd<sup>-</sup>-L, Pd<sup>-</sup>-L, and M(CO)<sub>5</sub>L complexes with L = CH<sub>3</sub>, CF<sub>3</sub>, SiH<sub>3</sub>, and SiF<sub>3</sub>. We have included the anionic Pd complexes because they have the same metal center and the same formal d<sup>10</sup> electron count as for the compounds in Table 1. The neutral Mn and Tc metal M(CO)<sub>5</sub>L complexes have the same formal d<sup>6</sup> electron count as the complexes treated in Table 2 and are more experimentally relevant than the corresponding anionic Cr and Mo d<sup>6</sup> complexes would be. The results are presented in Table 4.

A comparison of the data in Table 4 with the data in Tables 1 and 2 shows that the CH<sub>3</sub><sup>-</sup>, SiH<sub>3</sub><sup>-</sup>, and SiF<sub>3</sub><sup>-</sup> ligands are weak  $\pi$  acceptors, similar in strength to the pyridine ligand and hence weaker than any of the phosphine ligands. The trifluoromethyl ligand has a larger  $\pi$  acceptor character, similar to that of the phosphine ligands PH<sub>3</sub>, PMe<sub>3</sub>, and PPh<sub>3</sub>. It is interesting to note that the effect of fluorine substitution is much weaker for SiF<sub>3</sub>. Qualitative proof of the existence of back-bonding in the Tc-(CO)<sub>5</sub>CF<sub>3</sub> complex is given by the density difference (Fukui) function, as shown in the Supporting Information. The increased population of the  $\sigma^*$  C-F orbital due to back-bonding toward the CF<sub>3</sub> ligand would explain the weakening and consequently the activation of these otherwise unreactive C-F bonds by metal centers, as is observed experimentally.<sup>50</sup> As for the data in Table 2, decreased back-bonding is observed toward the L ligand in the L'-Pd-L complexes, where L' is a strong  $\pi$  acceptor, due to the competition for back-bonding from the same metal d orbital between the L and L' ligand.

Table 5 shows the total second-order perturbative interaction between the metal d<sub>yz</sub> orbital and the degenerate  $\sigma^*$  Y-X orbitals (as for the corresponding data in Table 3, the ligand orbitals having significant interaction with the metal d<sub>yz</sub> orbital are the two degenerate  $\sigma^*$  Y-X orbitals not lying in the xz

(44) Bennett, M. A.; Chee, H.; Jeffery, J. C.; Robertson, G. B. *Inorg. Chem.* **1979**, *18*, 1071.

(45) Graham, W. A. G. *Inorg. Chem.* **1968**, *7*, 315-321.

(46) Lichtenberger, D. L.; Rai-Chaudhuri, A. *J. Am. Chem. Soc.* **1991**, *113*, 2923-2930.

(47) Choi, S.; Lin, Z. *Organometallics* **1999**, *18*, 5488-5495.

(48) Lemke, F. R.; Galat, K. J.; Youngs, W. J. *Organometallics* **1999**, *18*, 1419-1429.

(49) Hübler, K.; Hunt, P. A.; Maddock, S. M.; Rickard, C. E. F.; Roper, W. R.; Salter, D. M.; Schwerdtfeger, P.; Wright, L. *J. Organometallics* **1997**, *16*, 5076-5083.

(50) (a) Torrens, H. *Coord. Chem. Rev.* **2005**, *249*, 1957-1985. (b) Kiplinger, J. L.; Richmond, T. G.; Osterberg, C. E. *Chem. Rev.* **1994**, *94*, 373-431.

**Table 5. Total Second-Order Perturbative Interaction between the Metal  $d_{yz}/\sigma^*$  Y–X Orbitals, Energy of the Respective Orbitals ( $\epsilon$   $d_{yz}$  and  $\epsilon$   $\sigma^*$ ), Energy Difference between These Orbitals ( $\Delta\epsilon$ ), and Off-Diagonal NBO Fock Matrix Element  $F(i,j)$  (kcal/mol)**

L	M	$E(2)$	$\epsilon$ $d_{yz}$	$\epsilon$ $\sigma^*$	$\Delta\epsilon$	$F(i,j)$
CH <sub>3</sub>	Mn	0.10	−151.8	294.9	446.8	3.8
	Tc	0.42	−143.1	296.8	439.9	7.5
CF <sub>3</sub>	Mn	1.40	−163.8	136.2	299.9	10.7
	Tc	2.64	−154.4	139.3	293.7	14.4
SiH <sub>3</sub>	Mn	0.44	−160.0	147.5	307.5	6.3
	Tc	0.38	−151.9	151.2	303.1	5.6
SiF <sub>3</sub>	Mn	0.84	−170.7	127.4	298.1	8.2
	Tc	0.72	−161.9	128.6	290.5	7.5

plane), the respective energy of these NBO orbitals, their difference in energy, and the off-diagonal NBO Fock matrix element  $F(i,j)$  for the Tc(CO)<sub>5</sub>L and Mn(CO)<sub>5</sub>L molecules. The molecules lie with the M–Y bond in the plane of the paper along the vertical  $z$ -axis, with the  $xz$  plane bisecting the carbonyl ligands and containing one of the Y–X bonds. This table shows that the  $\sigma$ -only character of the CH<sub>3</sub> ligand is mainly due to the large energy difference between the interacting orbitals. The energetically high  $\sigma^*$  C–H orbitals are clearly unsuitable for back-bonding. In the CF<sub>3</sub> ligand on the other hand, low-lying  $\sigma^*$  C–F orbitals are observed, which will lead to a smaller energy gap between the interacting orbitals. The  $\sigma^*$  orbitals are also more polarized toward the carbon atom than in the CH<sub>3</sub> ligand, which leads to better overlap with the metal donor orbitals; together with the more favorable energy gap, this explains the enhanced  $\pi$  acceptor character. The metal d orbitals of the fourth period Tc atom are higher in energy and larger in size than those in the Mn compounds, which leads to a smaller energy gap and a better overlap between the donor and acceptor orbitals for the two carbon-based ligands. This in turn explains the more extensive back-bonding in the Tc(CO)<sub>5</sub>CX<sub>3</sub> species compared to the Mn(CO)<sub>5</sub>CX<sub>3</sub> molecules.

Given these trends, the back-bonding for the SiH<sub>3</sub> and SiF<sub>3</sub> ligands is perhaps surprisingly low. The  $\sigma^*$  orbitals on these ligands are quite low in energy, with a gap to the donor orbitals comparable to that observed with the trifluoromethyl ligand. However, overlap of the  $\sigma^*$  orbitals with the metal donor orbitals is clearly not nearly as good as with the CF<sub>3</sub> ligand, as shown by the relatively small  $F(i,j)$  coupling matrix elements.

**C. Comparison of NBO with Other Methods for Assessing  $\Delta E_{bb}$ .** Various other methods have been used to assess the importance of back-bonding and other aspects of bonding, and these are in some sense complementary. For example, the NBO approach used here cannot simultaneously assess the strength of the  $\pi$  back-bonding interaction considered here and that of the  $\sigma$  donation, whereas other methods can. A very widely used method is the extended transition state (ETS) energy decomposition scheme,<sup>16</sup> one of the first applications of which<sup>16c</sup> was to the description of back-bonding to ligands such as CO and PF<sub>3</sub>. In the ETS method, the total energy change upon bond formation is decomposed into a number of contributions,  $\Delta E_{prep} + \Delta E_{elstat} + \Delta E_{Pauli} + \Delta E_{orb}$ , corresponding to “preparation” of the fragments for bonding (e.g., geometry changes between the free fragment and the molecule), electrostatic interactions between the unperturbed fragments, Pauli antisymmetrization, and orbital relaxation or bonding. This last term is due to covalent bonding and can be obtained for each irreducible representation of the molecular point group, allowing  $\sigma$  and  $\pi$  bonding for systems with the required symmetry to be assessed separately.

As noted in the Introduction, this ETS analysis has already been used for the M(CO)<sub>5</sub>PR<sub>3</sub> complexes (M = Cr, Mo), leading

**Table 6. Back-Bonding Interaction  $\Delta E_{bb}$  (kcal/mol) toward the YH<sub>3</sub> Ligand in Neutral and Cationic M(CO)<sub>5</sub>YH<sub>3</sub> Complexes Estimated by the ETS Scheme and a NBO Second-Order Perturbative Analysis**

mol. charge	method	M = Cr Y = N	M = Mo Y = N	M = Cr Y = P	M = Mo Y = P
0	ETS	4.52	3.88	14.56	13.54
0	NBO	0.37	0.79	4.37	6.56
1	ETS	6.88	6.54	13.48	13.12
1	NBO	0.00	0.00	1.48	2.67

to the conclusion that phosphines are bonded to a large extent by  $\pi$  interactions.<sup>18</sup> We have repeated these calculations for the PH<sub>3</sub> complexes, obtaining similar results. The slight differences between our results and those previously reported are due to small differences in geometry as well as to the use of a different basis set.

We have also carried out the ETS analysis on the analogous NH<sub>3</sub> species as well as the singly oxidized<sup>51</sup> derivatives of the PH<sub>3</sub> and NH<sub>3</sub> complexes. For all cases, the M–Y (Y = N, P) axis is taken as the  $z$ -axis, and the  $xz$  plane bisects the carbonyl ligands and contains one of the Y–H bonds. The six d electrons are thereby contained in the  $d_{yz}$ ,  $d_{xz}$ , and  $d_{x^2-y^2}$  metal orbitals which belong to the  $a''$ ,  $a'$ , and  $a'$  irreducible representations, respectively. The first two of these orbitals participate in  $\pi$  back-bonding interactions toward the  $\pi$ -symmetry linear combinations of the  $\sigma^*$  orbitals of the YH<sub>3</sub> ligand. Since one of these interactions involves orbitals within the  $a''$  irreducible representation, which is the case for no other important bonding interaction, one could assume as in the previous work<sup>18</sup> that the  $\pi$  back-bonding energy contribution is equal to twice the  $a''$  part of  $\Delta E_{orb}$ .

For the cationic systems, one of the key interactions between metal d and ligand  $\sigma^*$  orbitals involves a doubly occupied metal orbital, and the other one involves a singly occupied metal orbital. There are also two near-degenerate  $^2A'$  and  $^2A''$  states obtained after ionization from the  $a'$  ( $d_{xz}$ ) or  $a''$  ( $d_{yz}$ ) orbital, respectively. In the first case, the  $a''$  d orbital is doubly occupied (and the  $a'$  one singly occupied), and the reverse occurs in the other state. We have carried out separate ETS calculations on both states and estimate the overall back-bonding contribution  $\Delta E_{bb}$  for both of these molecules as being given by the sum of the  $\Delta E_{orb}$  term of  $a''$  symmetry in the two calculations. The results of the ETS analysis are summarized in Table 6 and compared to results obtained using NBO (some of the NBO results are taken from Table 2 and included again in Table 6 for convenience).

From Table 6, it is first of all clear that the ETS method attributes much higher absolute values to the  $\pi$  back-bonding interaction than the NBO analysis does. It also suggests that this interaction is stronger in the Cr than in the Mo complexes. Substantial back-bonding is also indicated toward the NH<sub>3</sub> ligands, with a  $\pi$  interaction close to half that obtained for the PH<sub>3</sub> ligand in some cases. In the NBO calculations, going from the neutral to the cation leads to a significant decrease in the strength of the back-bonding interaction. This is because of the loss of one electron from the donor orbital and because the increased charge leads to a lowering of the energy of all the donor d orbitals and to their contraction and hence to poorer overlap with the acceptor orbitals. Decreased back-bonding upon ionization is also shown by analysis of the Fukui function for these compounds.<sup>5</sup> In contrast, the ETS analysis does not show

(51) The bonding analysis for the cationic complexes is carried out at the same geometry as for the neutral species (see ref 5 for a discussion of the difference in their optimum geometries).

**Table 7.** Energy Stabilization (kcal/mol) Due to Back-Bonding  $\Delta E_{bb}$  in Pd–PX<sub>3</sub> Complexes Estimated by the CSOV<sup>a</sup> and NBO Scheme

X	Me	H	OMe	F
CSOV	9.57	11.24	14.11	20.33
NBO	16.44	14.91	18.31	23.68

<sup>a</sup> The CSOV results are taken from ref 8.

a substantial change in the strength of back-bonding upon ionization. In fact, for the NH<sub>3</sub> ligand, there is even a predicted increase in back-bonding upon oxidation.<sup>52</sup> These trends in the ETS analysis are surprising in all respects (Cr vs Mo, N vs P, cation vs neutral), whereas the NBO analysis gives in each case the expected trend.

This relatively poorer behavior of the ETS scheme can among others<sup>53</sup> be attributed to the fact that  $\Delta E_{orb}$  contains not only covalent bonding effects but also intrafragment relaxation effects or polarization. This can be understood by examining the thermodynamic cycle used to determine  $\Delta E_{orb}$ . In this cycle, the  $\Delta E_{elstat}$  term is determined using the charge distributions of the interacting fragments, and thereby does not account for electrostatic effects due to orbital relaxation (e.g., polarization and charge transfer), which are instead included in the  $\Delta E_{orb}$  term. Also,  $\Delta E_{Pauli}$  is computed by evaluating the energy of the Slater determinant obtained through simple antisymmetrization of the fragment wavefunctions. Orbital relaxation—which contributes to  $\Delta E_{orb}$ —will occur within each fragment so as to relax the electron distribution toward this perturbation. For these reasons,  $\Delta E_{orb}$  is expected to overestimate the importance of covalent bonding effects and, in particular, can be seen to exaggerate the impact of  $\pi$  back-bonding in all the complexes considered in Table 6. Others have already noted the potential importance of these relaxation effects.<sup>54</sup>

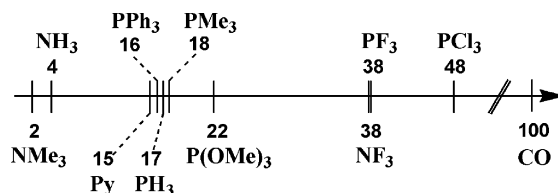
The constrained space orbital variation (CSOV) technique is another energy decomposition scheme used in the literature to estimate the strength of  $\pi$  back-bonding interactions.<sup>19</sup> Like the ETS method, the CSOV decomposes the bonding event into a number of steps that are assigned to individual contributions to the bond energy. The analysis starts from the superimposition and antisymmetrization of the frozen fragment wavefunctions (or Kohn–Sham densities) of the separated units. In a next step, the metal orbitals are fixed while the ligand orbitals are allowed to polarize, but only within the space of the ligand basis set. In a third step the virtual orbitals of the metal atom are included in the ligand variational space, allowing ligand to metal donation. The ligand orbitals obtained in this way are then fixed, and the metal orbitals are allowed to polarize in the metal basis set. Metal to ligand donation will be possible by adding the ligand virtual orbitals in the variational space of the metal. It is this last step that can be associated with back-bonding toward a phosphine ligand. In principle, this stepwise procedure should give bonding energies similar to a full, unconstrained calculation.

Table 7 shows the results of an earlier survey<sup>8</sup> using this method to estimate back-bonding in Pd–L complexes, as well as our results for these complexes given earlier in Table 1.

(52) The ETS scheme shows a loss in  $\pi$  bonding only if one considers the relative % of this type of bonding to the total bonding in these complexes, as can be seen from the Supporting Information. Upon ionization the % of  $\pi$  bonding decreases by 10% for the M(CO)<sub>5</sub>PH<sub>3</sub> complexes (from 35 to 25 %) and remains equal for the M(CO)<sub>5</sub>NH<sub>3</sub> complexes (about 20%).

(53) The  $\pi$  interaction estimated by the ETS method in Table 6 includes both the  $\pi$  back-bonding to the ligand and  $\pi$  donation from the ligand to the metal. An increase in the latter could in principle account for the increase in the ETS  $\pi$ -bonding energy. However, on the basis of the NBO analysis, these latter interactions are not important.

(54) Bartolotti, L. J.; Ayers, P. W. *J. Phys. Chem. A* **2005**, *109*, 1146.

**Figure 3.** Calculated  $\pi$  acceptor index for P- and N-based ligands.

Although the absolute values are in the same range, the NBO results indicate a slightly more important back-bonding interaction and indicate the PH<sub>3</sub> ligand to be a better  $\pi$  acceptor compared to the PMe<sub>3</sub> ligand. The opposite trend is found using the CSOV technique. However, the results are in better agreement with the NBO analysis than those obtained using the ETS approach, probably because the orbital relaxation effects within each fragment are treated separately from the bonding interactions in the CSOV method.

**D.  $\pi$ -Acceptor Index.** It is possible to combine the results obtained for the different metal complexes to obtain a single measure of  $\pi$  acceptor character for all these ligands. This is a necessarily arbitrary exercise, as there is no unique way to combine the results for all the metal complexes, but it provides a useful summary and a single scale on which to compare different ligands. In this case, we have chosen to add together the  $\Delta E_{bb}$  values for the NH<sub>3</sub>PdL, PdL, PH<sub>3</sub>PPdL, and COPdL complexes and to add to the resulting value 5 times the sum of the  $\Delta E_{bb}$  values for the Cr(CO)<sub>5</sub>L and Mo(CO)<sub>5</sub>L complexes. The factor of 5 is included so as to give an overall comparable weight to the smaller  $\Delta E_{bb}$  values calculated for the chromium and molybdenum species and the larger values obtained for the palladium complexes. The resulting value is then normalized to 100 for the strongest acceptor, CO. This gives the values shown in Figure 3. These results are broadly in line with the known properties of the ligands but provide a quantitative scale of back-bonding interactions for this range of ligands.

It is less straightforward to place the CX<sub>3</sub> and SiX<sub>3</sub> ligands on the same scale, as the change in metal, oxidation state, and/or charge for the results in Table 4 compared to those in Tables 1 and 2 makes a direct comparison difficult. However, to a first approximation, using the same additive scheme (the sum of the  $\Delta E_{bb}$  values for the Pd complexes plus 5 times the sum of the back-bonding energies obtained for the Mn and Tc compounds) yields values that are consistent with accepted chemical wisdom. Thus using this equation, the CH<sub>3</sub>, SiH<sub>3</sub>, and SiF<sub>3</sub> ligands appear as insignificant  $\pi$  acceptors ( $\pi$  acceptor indices of 5, 7, and 9, respectively), whereas the CF<sub>3</sub> ligand is a significant but still weak acceptor (15).

## Conclusion

A quantitative study of back-bonding toward YX<sub>3</sub> ligands (Y = P, N, C, Si; X = H, F, Me, Ph, OMe) is performed using NBO second-order perturbative energy analysis to estimate the interaction between the metal d and  $\sigma^*$  Y–X orbitals. Back-bonding toward N=C  $\pi^*$  orbitals for pyridine ligands is also considered. Care is needed to select a suitable Lewis structure reference in order to obtain useful orbital interaction energies. The results show that the NH<sub>3</sub> and NMe<sub>3</sub> ligands are essentially pure  $\sigma$  donors, with a very small  $\pi$  acceptor character. Pyridine and NF<sub>3</sub>, in contrast, are respectively found to be weak and strong  $\pi$  acceptors. PH<sub>3</sub>, PMe<sub>3</sub>, and PPh<sub>3</sub> are also weak  $\pi$  acceptors, the PF<sub>3</sub> and PCl<sub>3</sub> ligands are strong acceptors, and P(OMe)<sub>3</sub> is of intermediate character.

The NBO results furthermore show the existence of competitive back-bonding toward other ligands such as the CO ligand,



clearly indicating the latter ligand to be a stronger  $\pi$  acceptor than any of the phosphorus- or nitrogen-based ligands considered here. We also consider  $\text{CF}_3$  and  $\text{SiF}_3$  ligands, with the former showing some weak  $\pi$  acceptor character. The results show that the back-bonding effect depends not only on the difference in (metal) donor–(ligand) acceptor orbital energy but also on the effective overlap of these orbitals.

Comparing our NBO results with published and new extended transition state (ETS) analysis of bonding in  $\text{M}(\text{CO})_5(\text{YH}_3)^{0,+}$  ( $\text{M} = \text{Cr}, \text{Mo}$ ;  $\text{Y} = \text{N}, \text{P}$ ) neutral and cationic species shows that the ETS method overestimates the importance of  $\pi$  back-bonding in these species. This is most likely because large orbital relaxation effects within the metal fragment and the ligand occur upon addition of the ligand to the metal, as well as the specific bonding interactions considered here. This leads to unexpected and implausible results for the amine ligands and the cationic species. A description of the total metal–ligand bond will therefore benefit from a combination of a NBO as well as ETS analysis, both bringing complementary information.

Overall, a single scale of  $\pi$  acceptor character is proposed. Although this is a somewhat arbitrary combination of the calculated back-bonding energies for the different ligands, it

provides a convenient single number to characterize the different ligands. The resulting values are mostly in good agreement with chemical intuition but provide additional quantitative detail that can be of interest when designing new ligands or analyzing bonding in novel compounds.

**Acknowledgment.** The authors are indebted to the Belgian National Fund for Scientific Research (FNRS) for its financial support to this research (T.L. is Research Fellow, grant FC 64894). They would like also to thank the FNRS for its support to access computational facilities (FRFC project No. 2.4556.99 “Simulations numériques et traitement des données”). J.N.H. thanks the EPSRC for an Advanced Research Fellowship. ADF calculations were carried out using the UK EPSRC National Service for Computational Chemistry Software.

**Supporting Information Available:** Additional details of NBO and ETS analyses, plots of Fukui function for  $\text{Mo}(\text{CO})_5(\text{NF}_3)$  and  $\text{Tc}(\text{CO})_5(\text{CF}_3)$ , and optimized geometries of all species. This material is available free of charge via the Internet at <http://pubs.acs.org>.

OM061151Z